Environmental Science and Pollution Research (2023) 30:27965–27979
https://doi.org/10.1007/s11356-022-23982-x

RESEARCH ARTICLE

Mapping of dust source susceptibility by remote sensing and machine learning techniques (case study: Iran-Iraq border)

Sima Pourhashemi[1] · Mohammad Ali Zangane Asadi[1] · Mahdi Boroughani[2] · Hossein Azadi[3]

Received: 12 May 2022 / Accepted: 30 October 2022 / Published online: 17 November 2022

Abstract

A dust storm is a major environmental problem affecting many arid regions worldwide. The novel contribution of this study is combining indicators extracted from RS- and statistic-based predictive models to spatial mapping of land susceptibility to dust emissions in a very important dust source area in the borders of Iran and Iraq (Khuzestan province in Iran and Al-Basrah and Maysan provinces in Iraq). In this research, remote sensing (RS) techniques and machine learning techniques, including multivariate adaptive regression spline (MARS), random forest (RF), and logistic regression (LR), were used for dust source identification and susceptibility map preparation. To this end, 152 DSA for the period of 2005–2020 were identified in the study area. Of these DSA data, 70% was assigned to the Dust Source Susceptibility Mapping (DSSM) (training dataset) and 30% to model validation. Consequently, six factors (i.e., soil, lithology, slope, normalized vegetation differential index (NDVI), geomorphology, and land use units) were prepared as DSA's independent and effective variables. The results of all three models indicated that land use had the most impact on DSA. The validation results of these models using the test data showed sub-curves of 0.92, 0.86, and 0.76 for the RF, MARS, and LR models, respectively. Also, results showed that the RF model outperformed MARS (AUC = 0.89) and LR (AUC = 0.78) methods. In all three models, high and very high susceptibility classes generally covered a large percentage of the case study. The highest percentage of dust source points was also in this susceptibility category. Overall, the results of this study can be useful for planners and managers to control and reduce the risk of negative dust consequences.

Keywords Dust storm · Multivariate adaptive regression spline (MARS) · Random forest (RF) · Logistic regression (LR)

Introduction

A dust storm is a catastrophic weather phenomenon with adverse effects on the quality of the environment and cause significant damage to health, agricultural products, and the economy (Guo et al. 2018; Liu et al. 2020). Strong winds are the greatest cause of dust events, and soil surface properties such as vegetation distribution, surface roughness, soil texture, and moisture have important effects on dust emissions (Shaheen et al. 2020). The dust source points are located in areas with less than 300 mm of rainfall in the world (Wang et al. 2016; Al-Dousari et al. 2017; Kandakji et al. 2021). When wind speeds in dry areas and deserts exceed the wind erosion threshold (6.5 to 7 m/s), soil particles rise and dust storms occur (Namdari et al. 2021). Dust particles can reach a height of 6 km above the ground and be transported up to a distance of 20,000 km (Taheri et al. 2020). Dust storms in arid and semi-arid regions affect the amount of solar radiation, air pollution, horizontal vision, enzymatic activities,

Responsible Editor: Philippe Garrigues

✉ Mohammad Ali Zangane Asadi
ma.zanganehasadi@hsu.ac.ir

Sima Pourhashemi
s_pourhashemi@yahoo.com

Mahdi Boroughani
m.boroughani@hsu.ac.ir

Hossein Azadi
hossein.azadi@ugent.be

[1] Department of Geography, Hakim Sabzevari University, Sabzevar, Iran

[2] Research Center for Geosciences and Social Studies, Hakim Sabzevari University, Sabzevar, Iran

[3] Department of Geography, Ghent University, Ghent, Belgium

agricultural lands, and human health (Boroughani et al. 2022; Martinich et al. 2019; Yang et al. 2018). In recent years, the frequency of days with dust storms has increased significantly due to drought and Land Use Change (LUC). As a result, agriculture, industry, and society have experienced adverse biological effects and extensive damage (Heald and Spracklen 2015). The combined development of this event along with the accelerated trend of development, industrialization, and population growth in urban areas has doubled the environmental tensions (Shaheen et al. 2020; Boloorani et al. 2020). Dust storms occur in the world's arid lands, especially in North Africa and the Middle East (Yu et al. 2015; Francis et al. 2021). These storms reduce visibility and lead to serious environmental, socio-economic, and health issues (Middleton 2017). The Middle East faces severe environmental challenges, such as climate and environmental changes caused by human activities (Karimi and Samadi 2019). The root cause for the increase in dust in the region is the severe destruction of natural resources due to extensive exploitation, drying of wetlands, dam construction, and the continuation of the drought in the last decade (Cao et al. 2015). Identifying areas of dust origin using remote sensing techniques is one of the main important methods in the literature (Jiao et al. 2021). Much research has been conducted on determining dust detection using RS techniques. In most of these studies, MODIS images and dust detection indices (BTD2931, BTD3132, NDDI, parameters D, and DEP) are used to identify dust in the Saharan Desert (Schepanski et al. 2012; Feuerstein and Schepanski 2019), Chihuahuan Desert (Baddock et al. 2016), Iran (Rahmati et al. 2020), Khorasan Razavi Province, Urmia Lake and Sistan watershed, Iran (Boroughani et al. 2019, 2020, 2021), Middle East (Namdari et al. 2018), India (Soni et al. 2018), the USA and Middle East (Miller 2003), and Southwestern North America (Lee et al. 2009). Data mining is an important method for mapping environmental and natural hazards. This technique is employed to find new and useful data from a large body of information (Gholami et al. 2020a). Numerous studies (e.g., Hong et al. 2016; Dube et al. 2014; Manap et al. 2014; Rahmati et al. 2020; Lin et al. 2020; Boroughani et al. 2020, 2021, 2022; Gholami et al. 2020b; Lee et al. 2021; Gholami et al. 2021) have used a data mining approach using different algorithms and models to identify and generate susceptibility maps of dust, landslide, groundwater, fire, flood, and gall erosion centers. The concept of data mining includes algorithms and methods that are used to extract information from important data (Akbari et al 2017).

Considering the intensity and a large number of dust storms in the case study (i.e., Iran and Iraq border) and their importance, this study aims to identify dust sources and generate a susceptibility map using these algorithms. The main objectives of this study are (i) identifying the sources of dust with remote sensing techniques; (ii) generating dust susceptibility mapping using MARS, RF, and LR algorithms; (iii) comparing the accuracy of model outputs using statistical evaluation criteria; and (iv) determining the importance of each ventilation agent in the potential of the dust source.

Methodology

Setting of the study

The research area covers Khuzestan province in Iran and Al-Basrah and Maysan provinces in Iraq with an area of 99,494.38 km^2 (Fig. 1). The highest and lowest elevations in the study area are 3676 and − 37 m.a.s.l, respectively. Al-Hawizeh/Al-Azim Marsh, located on the border between Iraq and Iran, is known as one of the main dust sources in Iran. The mean annual temperature is 26℃ and the average annual precipitation is less than 250 mm per year in the area. According to Javadian et al. (2019), Al-Howizeh/Al-Azim Marshes are among the greatest important dust sources in Ahvaz city. Wetlands in Iran in the last decade have dried up and created a source of dust due to oil extraction around Al-Azim (Arkian 2017). Several other factors (e.g., climate change, drought, wars in the region and military operations, surface water control, river diversion, and dam construction projects) have accelerated to the destruction of these wetlands and the emergence of their surface as dust source (Cao et al. 2015; Rashki et al. 2021). The Khuzestan Plain, which forms a large part of Khuzestan Province in southwestern Iran, contains much small dust sources. Approximately 9% of the Khuzestan plain has the potential to produce dust, and a part of this plain is sensitive to the dust source of the Al-Azim dried-up swamp (Heidarian et al. 2018(. These source areas contain degraded pastures, abandoned rainfed farmlands and irrigation fields, and temporary salt lakes. Among these salt lakes, we can mention Maleh Playa, Sabzeh Zohreh Sharghi, and Sabkha Karun Gharbi (Abyat et al. 2019).

Figure 2 presents the two main stages of conducting the present research. First, DSA was determined using satellite images (i.e., MODIS) and dust detection indices. In the second stage, sensitivity maps were prepared by six environmental forecasters, the DSA was extracted from satellite images and three machine learning algorithms (i.e., logistic regression, random forest, and MARS model) were examined. In the following, the working method and dataset are explained in detail.

Dust source identification

This study collected MODIS sensor images from Terra and Aqua satellites (Vickery and Eckardt 2013). Initially,

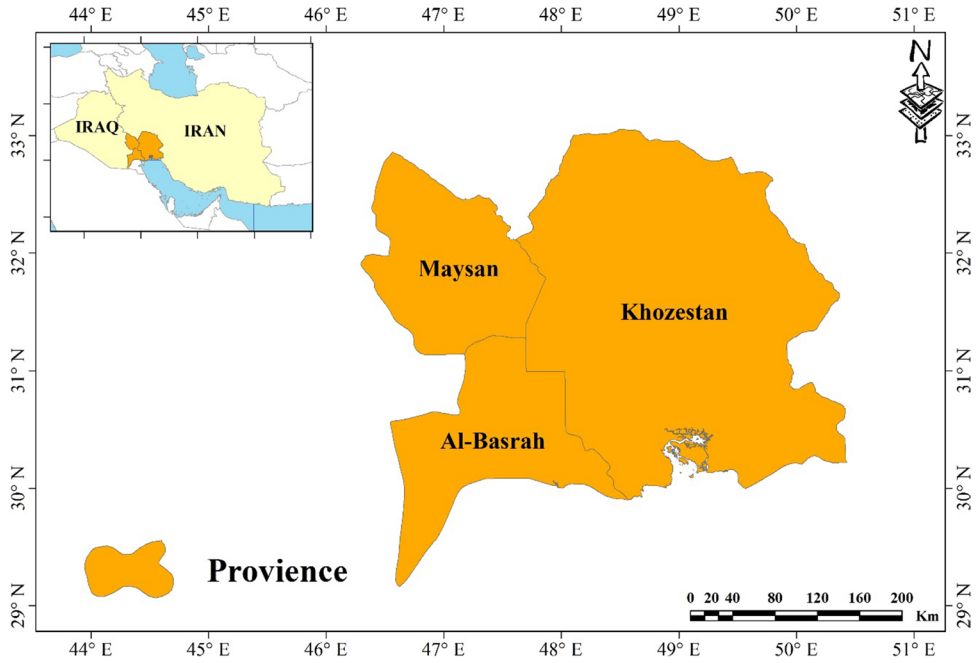

Fig. 1 Location of the research area

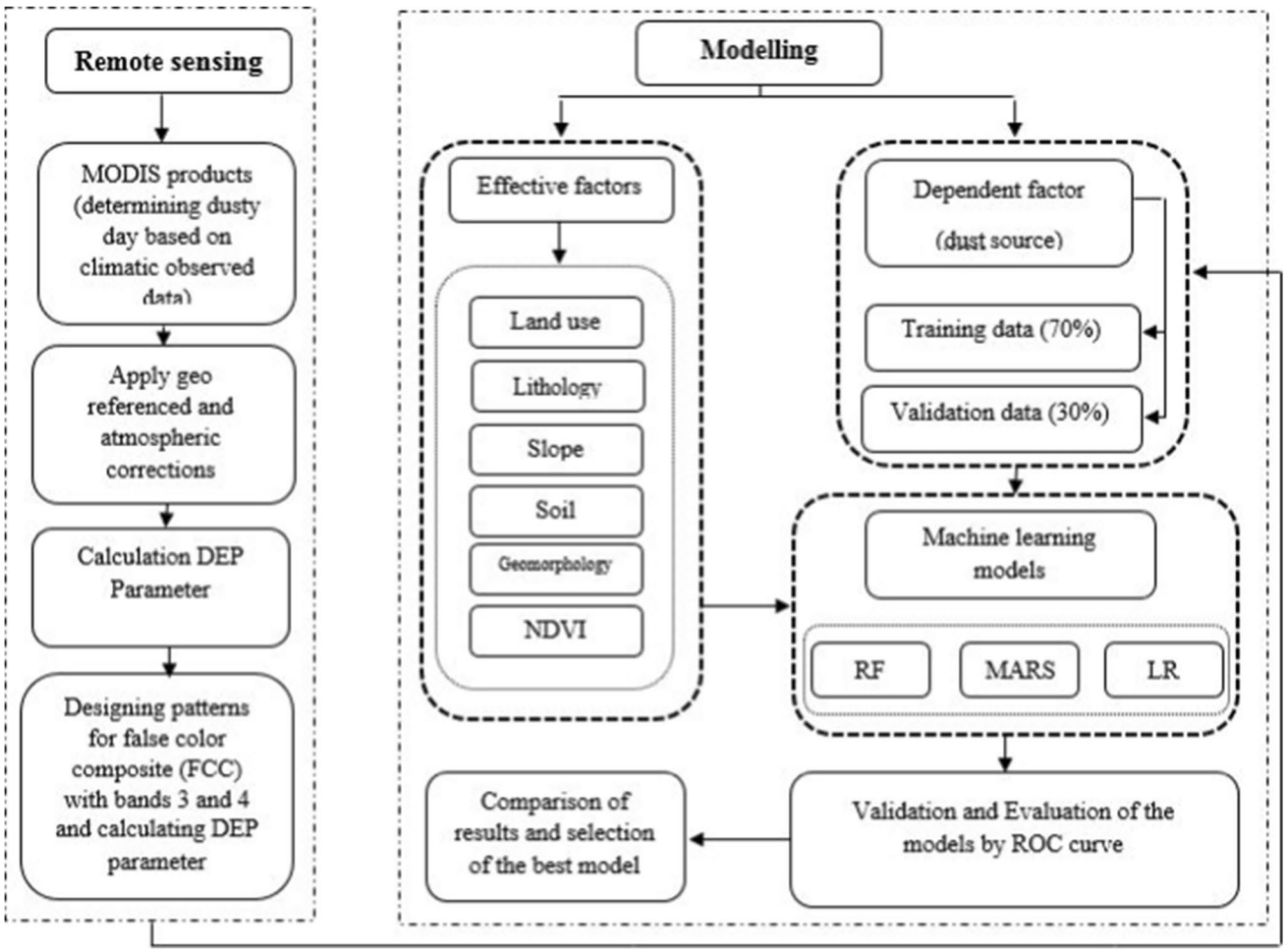

Fig. 2 Flowchart for preparation of dust susceptibility maps using LR, MARS, and RF models

the days of dust occurrence from 2005 to 2020 were determined using meteorological data, such as visibility less than 2000 m, wind speed above 7 m per second, and cloudy conditions. Then, the days when the occurrence of dust coincided with the imaging were determined. Finally, 31 MODIS sensor images were used by the Terra satellite related to the selected dust days from 2005 to 2020.

MODIS images were selected for their several advantages, including free access, high spatial resolution (LAADS Alerts 2021), and wide view (Hahnenberger and Nicoll 2014; Lee et al. 2021). The dust Detection Products (DEP) or the Miller method was calculated for all satellite images to identify (Miller 2003). Finally, false-color combinations were used to identify dust storms. These instructions were according to the DEP plus bands 3 and 4 of MODIS images. The false-color combinations included DEP (Miller 2003), B4, and B3. A Gaussian columnar model was used to detect dust. This technique is developed on a cone of dust diffusion viewed in the processed MODIS images, where the apex shows the source of the dust (Walker et al. 2009; Lee et al. 2009).

Dust source effective factors

Quantifying the relative significance of the factors influencing the area's dust source is essential to understanding the dust cycle (Kok et al. 2017). The DSA potential map was prepared using six factors (i.e., soil map, lithology, slope, vegetation index (NDVI), geomorphology units, and land use) in the model after preparing the DSA distribution map. These factors play the most important roles in creating DSA (Kandakji et al. 2020). Since measured wind-speed data were unavailable at Iraq stations, we limited the research by examining the effect of topographic variables. The effect of wind on land susceptibility to wind erosion was previously examined in the Great Salt Desert in Iran using availabile wind speed data (Boroughani et al. 2022).

Dust storms are more likely to occur in regions with erosion-sensitive lithological units than in areas with resistant units (Francis et al. 2017). Lithology classes have significant effects on dust storms and occur more in regions susceptible to lithology than in regions with dust storm-resistant units (Francis et al. 2017). In the study, the geological map of the research area was prepared using the world geological map at a scale of 1: 250,000. Also, lithological units were obtained from the map in 6 classes Siltstone and Marne, dolomitic limestone and clay, limestone, conglomerate, river sediments, and wind sand (Fig. 3a). Soil physical characteristics control the dust storms, and the amount of dust raised (Alilou et al. 2019; Rahmati et al. 2020). Vegetation-free soils are erosion-sensitive areas with high dust production capacity (Gholami et al. 2020a). In this study, 6 main types of floors, including Clay-Loam, Loam, Loamy-Sand, Sandy-Loam, Sand, and Salty-Clay, were identified (Fig. 3b).

Plain and flatlands with low slopes have a better potential for dust generation and wind erosion than steep lands. In these regions, the wind quickly reaches the wind erosion threshold, leading to dust storms (Wu et al. 2016). Using the DEM of 30 m, the slope map of the research area was prepared in six classes (Fig. 3c). In many studies (e.g., Lee and Sohn 2011), a negative relationship was established between vegetation and the number of dust storms by analyzing the spatial and long-term vegetation changes. The vegetation can absorb wind energy, increase ground roughness, and protect soil from wind erosion (Feng and Janssen 2018). The Normalized Difference Vegetation Index (NDVI) was used to prepare the vegetation map of the area. ETM^{+} images of the Landsat 8 satellite (related to 2019) were used for this goal. Based on the NDVI values, the study area was zoned into 3 vegetation classes, including -0.0196 to 0, 0 to 0.025, and $0.025 <$ (Fig. 3d).

Land use is strongly associated with dust storms; for example, a lack of vegetation and degraded soil crust has a greater capacity to produce dust (Goossens and Buck 2014). The land use map was prepared using Landsat 8 satellite images for the summer of 2018, as the highest amount of dust occurs in this period. The land use map was classified into Agriculture land. Bare land, Forest, Marshland, Residential Area, Shrub Cover, Sparse Shrub Cover, and Wetland. (Fig. 3e).

Soil particles released into the air are closely related to the geomorphological characteristics of DSA. (Lee et al. 2021). The map of geomorphology units was prepared using slope and topographic maps with an accuracy of 1: 50,000 and the geology of the research area. In the next step, after interpreting the satellite images of Google Earth and Landsat 8 in 2017, more detailed information was extracted and transferred to the initial map. Finally, the map of the geomorphological units of the region in six classes was prepared (Fig. 3f).

Modeling

This research conducted a multi-collinearity analysis to examine alignment and make a preliminary study among independent variables. If there are several lines between independent variables, the error increases, and the accuracy of the model prediction decreases (Park et al. 2017). Two indicators (i.e., a tolerance of ≤ 0.01 and a variance coefficient of ≥ 10 indicating alignment) were used to examine the alignment between the independent variables (O'Brien 2007).

The first step for modeling is to prepare an educational data set and validation (Boroughani et al, 2020). To this end, the dust source was divided into two groups of 70% (106

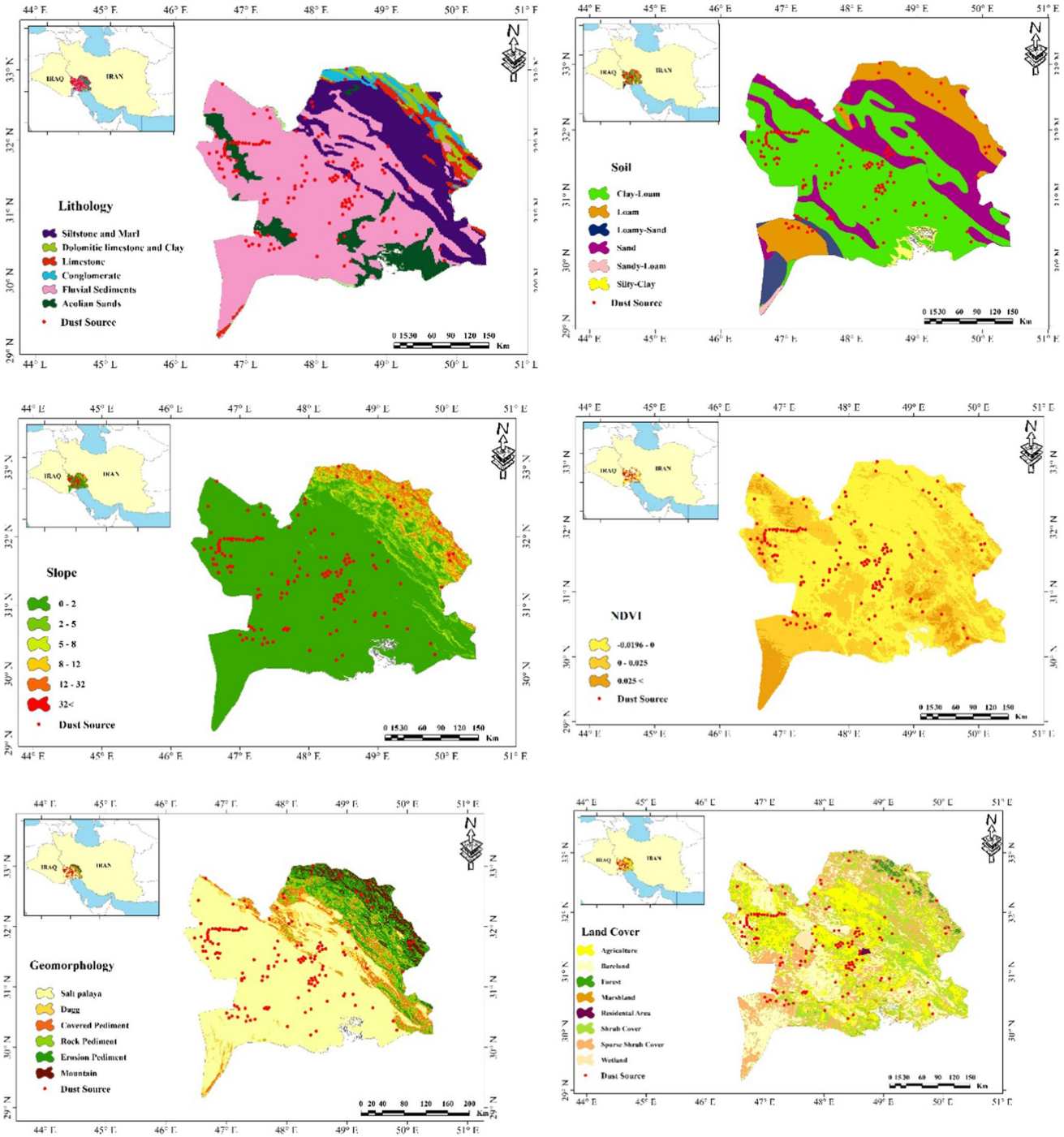

Fig. 3 Map of effective factors of dust source

dust sources) for modeling and 30% (46 dust sources) for evaluation (validation) using the stratified random sampling method (Lee et al. 2021) DSA sensitivity to data mining algorithms and the number of DSA in the area were analyzed by extracting the number of points without the DSA randomly. In the next step, the data related to the effective factors in the area of dust source and source distribution map were imported to the R software and analyzed using, and LR, MARS, and RF algorithms using different packages (e.g., glm, earth, and random forest). Afterword, dust source susceptibility was calculated for each pixel in the study area. Finally, the results were transferred to the ARC MAP 10.5 environment to produce a dust susceptibility map. In the following, these algorithms are described briefly.

Logistic regression (LR)

LR is a nonlinear mathematical model for determining the relationship between a binary dependent variable and several independent variables (Crawford et al. 2021). In this research, the most effective factors in DSA were investigated using LR. The model output should have coefficients between 0 and 1, which through logit theory gives probabilities higher than 0.5 value of 1 (affecting the DSA) and less than 0.5 value of zero (without the effect of the DSA) (Martinez-Garcia et al. 2011; Chen and Chen 2021).

The logistic model in the simplest form can be expressed as Eq. 2:

$$P = \frac{1}{1 + e^{-z}} \tag{2}$$

where P is the possibility of an occurrence of an event (DSA), the value of which varies from 0 to 1 in an S-shaped curve. Also, Z is defined as an equation (linear logistic model) whose value varies from -∞ to + ∞ (Wang et al. 2021a). This parameter is expressed by Eq. (4) as follows 3 (Nhu et al. 2020):

$$Y = \text{Logit}(p) = \ln\left(\frac{p}{1-p}\right) = C_0 + C_1X_1 + C_2X_2 + \cdots + C_nX_n \tag{3}$$

where P is the probability of DSA occurrence; X is the so-called odds ratio or probability, the width of the source or a constant coefficient, and C1, C2,… Cn are the coefficients of the independent variables (X1, X2,…, Xn). This model analyzes the presence or absence of dependent variables (DSA) to independent variables (Crawford et al. 2021).

Random forest (RF) model

RF is one of the best learning algorithms (Schonlau and Zou 2020) that performs high-accuracy classification for many datasets (Lee-Sunmin et al. 2017). Another positive feature of RF is that it works very well with huge data records (Jiang et al. 2021). RF classification was performed initially on educational information and on validation confirmation information (Schonlau and Zou 2020; Quevedo et al. 2021). Finally, the model with the lowest Out of Bag (OOB) error was chosen. The influence of each controlling factor in RF was determined using two factors of Mean Decrease Accuracy and Gini mean reduction (Wu et al. 2021).

Multivariate adaptive regression spline model (MARS)

MARS is one of the local nonparametric models first proposed by Friedman (Wang et al. 2021b). In this method, regression models create flexibility for dividing the response space into intervals of input variables and fitting a base pan (Spline) (Wang et al. 2020; Friedman 1991). This method is based on functions called base functions (functions that are used to display information in one or more variables), which are defined for each variable as follows:

$$\text{Y} = \max(0, \text{x} - t)\text{and}\text{Y} = \max(0, \text{t} - \text{x}) \tag{4}$$

which is t reached a Knot and is a threshold value. These functions are called spline functions, where t pairs are reflected in a node. The general shape of the MARS model is defined as follows (Roy et al. 2020):

$$\widehat{Y} = \text{f}(X) + c_0 + \sum_{k=1}^{M} c_k B_k(X) \tag{5}$$

where 5 Y is the value of the objective parameters defined by the function f (X), B_k (i.e., the base function) and the coefficients c_k (which are determined by minimizing the sum of the remaining squares). In the second step, the basic functions that are less important and effective in estimating are removed. Finally, the best model is chosen based on the minimum criterion called generalized cross-validation (GCV). GCV is used to identify the sub-models with the least effect on modeling.

If GCV_k is the value of GCV for the k model in the elimination phase, the GCV on which the best adaptive multiple spline regression models is selected is as follows (Martinello et al. 2021; Hassangavyar et al. 2020):

$$GCV_k = \frac{1}{n}\sum_{i=1}^{n}\left(y_i - \widehat{f}_k(x_i)\right)^2 / \left(1 - \frac{C(k)}{n}\right)^2 \tag{6}$$

where $\widehat{f}_k$ model is estimated in step k of the regression elimination stage and $\lambda.m$ + number of model sentences in step k = $C(k)$

Here, m represents the number of nodes of the linear functions in the model and λ is the smoothing parameter, which is usually chosen between 2 and 4.

Evaluation of dust source susceptibility map

One of the most important parts of modeling is validating the prediction outputs (Shano et al. 2021). In this research, all identified DSAs were separated into two parts: 70% for training and 30% for validation. DSAs were selected based on random logic for the training and validation of models. The receiver-operating characteristic-area below the curve (ROC-AUC) and the root mean square error RMSE were used to evaluate the accuracy of the statistical model. The ideal model has the highest subsurface level and its value is between 0.5 to 1 (Nandi and Shakoor 2010). The closer the surface below the curve is to 1, the more accurate the zoning map will be (Hao et al. 2020). Qualitative-quantitative

correlation should be below the curve and estimation of the 0.9–1, excellent; 0.8–0.9, very good; 0.7–0.8, good; 0.6–0.7, average; 0.5–0.6, weak is suggested (Arabameri et al. 2021). The ROC curve was used in this study to assess the performance of the generated susceptibility map. However, some studies suggest that model performance evaluation using a factor such as AUC may not be appropriate because in some cases high AUCs may not guarantee the high accuracy of spatial predictions (Chaudhary et al. 2021). For such cases, RMSE measurements are also used as additional criteria for evaluating model predictions and supporting decisions in model selection.

Result and discussion

Dust source identification

A total of 152 DSAs (77 in Iran and 75 in Iraq) were identified throughout the examined region (Fig. 4). The analysis was based on the results of previous studies that used RS techniques for identifying DSA in some parts of the world (Walker et al. 2009; Miller 2003; Hahnenberger and Nicoll 2014; Boroughani et al. 2020, 2021, 2022). These studies identified dust storm sources using DEP and dust enhancement indicators. Figure 5 presents dust detection from the MODIS FCC satellite imagery over the case study on 17 June 2008.

The results of the multilinear test (Table 1) confirmed that there was no agreement between the effective factors (independent variables); therefore, all layers were used for modeling.

Dust source susceptibility modeling

The DSSM was done in the research area based on the coefficients obtained for independent variables through the model implementation (Table 2). Table 3 presents the logistic regression model results to investigate the most important factor affecting the creation of DSA. Based on the obtained results, land use has the greatest impact on DSA creation, while geomorphology, soil, and vegetation index are placed in the next priorities. Negative coefficients indicate the inverse relationship of the dependent variable (DSA) with independent variables. Negative coefficients indicate a weak correlation than other factors. In this study, the lithological factor had the least impact on forming these DSAs. Also, the Hosmer and Lemeshow test and the Negelkerke coefficient were used to evaluate the validity of the model and the fit of the estimated pattern. In the Hosmer and Lemeshow test, the model is valid if the significance of the obtained model is more than 0.05 (Gomila 2021). Since the probability of the Hosmer and Lemeshow test statistic is 0.158, which is greater than 0.05, this value indicates the adequacy of the data for the model suitability.

In the Nagelkerke coefficient of determination method, the closer this value is to 1, the more the model corresponds to reality (Zhang et al. 2021). The value of the Cox and Snell coefficient of determination ($R^2_{\text{Cox\&Snell}}$) is 0.4312, which is significant in practice. The results of this model are shown in Table 2.

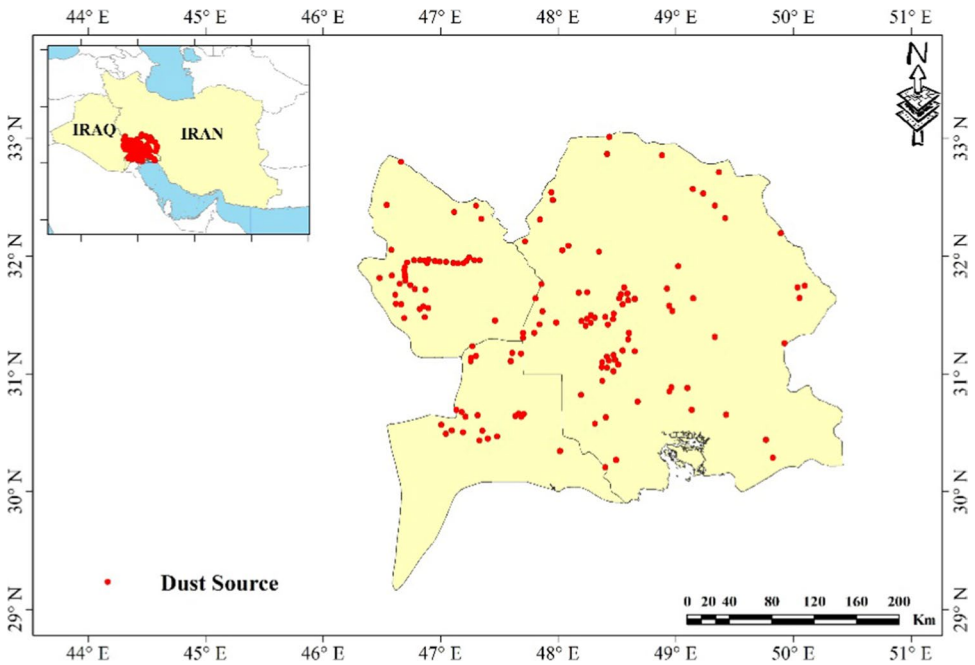

Fig. 4 Distribution of dust sources area identified

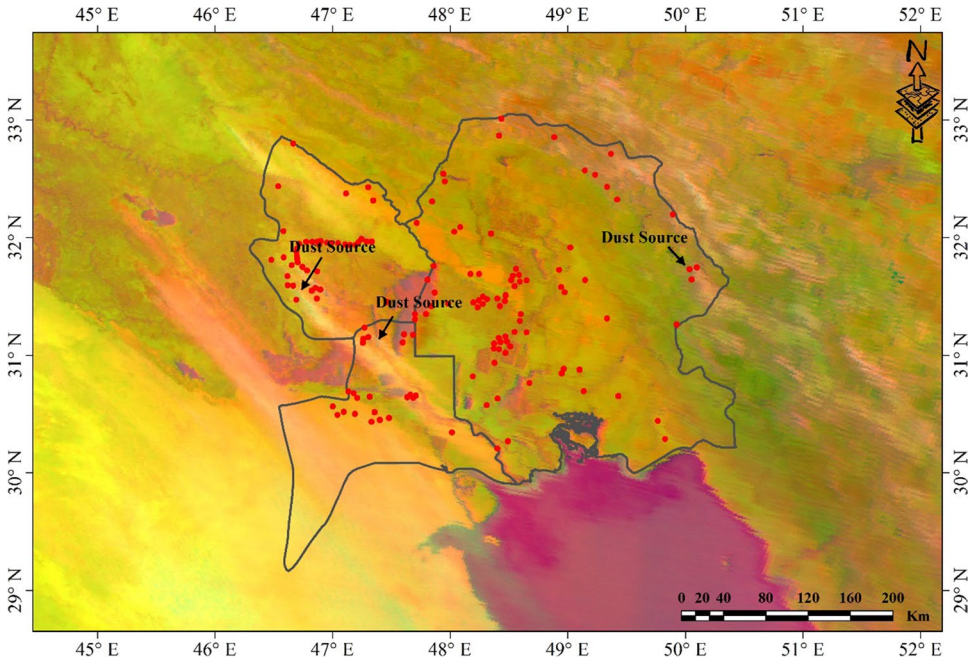

Fig. 5 Dust detection in the case study from the MODIS satellite Imagery with FCC (R: DEP, G: B4, B: B3)

Table 1 Multicollinearity diagnostic indices for effective factors

Factors	Tolerance	VIF
Slope	.236	4.239
Geomorphology	.241	4.144
Land use	.793	1.262
Lithology	.456	2.191
Soil	.539	1.855
NDVI	.454	2.201

Source: Study findings

Table 2 Model summary

-2 Log likelihood	Cox & Snell R^2	Nagelkerke R^2
471.3[a]	.43	.42

Source: Study findings

Table 3 Coefficients of independent logistic regression statistical analysis

Variables	B	Wald	Sig	Exp(B)
Soil	− .599	7.161	.007	.550
geomorphology	.674	7.923	.005	1.963
Land use	− .933	25.653	.000	.393
Lithology	− .163	.782	.037	.849
Slope	− .383	2.946	.086	.682
NDVI	− .270	.960	.032	.763

Source: Study findings

The results of the relationship between DSA and effective factors using the RF model are shown in Table 5 and Fig. 6. As previously mentioned, two factors of the Gini significance index and Mean Decrease Accuracy were used to determine the priority of each of the effective factors in creating DSA. Figure 6 shows the results of prioritizing the effective variables for the RF model using two criteria of Mean Decrease Accuracy and Gini significance index. The results of both criteria showed that the three factors of land use, soil, and geomorphology have the greatest effect on DSA. In most studies conducted in different parts of the world, these three factors have been identified as the most effective factors in creating DSA (Genuer et al. 2017; Giang et al. 2020; Ebrahimi-Khusfi et al. 2021). Boroughani et al. (2020) found that land use and geomorphology had a major influence on the DSA in Khorasan Razavi province in Iran.

The OOB results show a predicted error rate of about 22.17% and an accuracy of 77.83%. Based on the results of Table 4, the model incorrectly predicted 9 cases in the absence of DSA (row 1) in the presence of DSA (error 1), and the section Existence of DSA predicted 11 cases in the column of the absence of DSA (error 2). Besides, the model correctly predicted the absence of DSA for 97 cases and the presence of DSA for 95 cases.

The results of the MARS method were used to evaluate the factors affecting the establishment of a dust source area. The main difference between this method and conventional methods is that the former determines the effective variables, while the later determines the dependent variable versus the independent variable. The MARS analysis is performed after fitting the model to the data with different settings. These

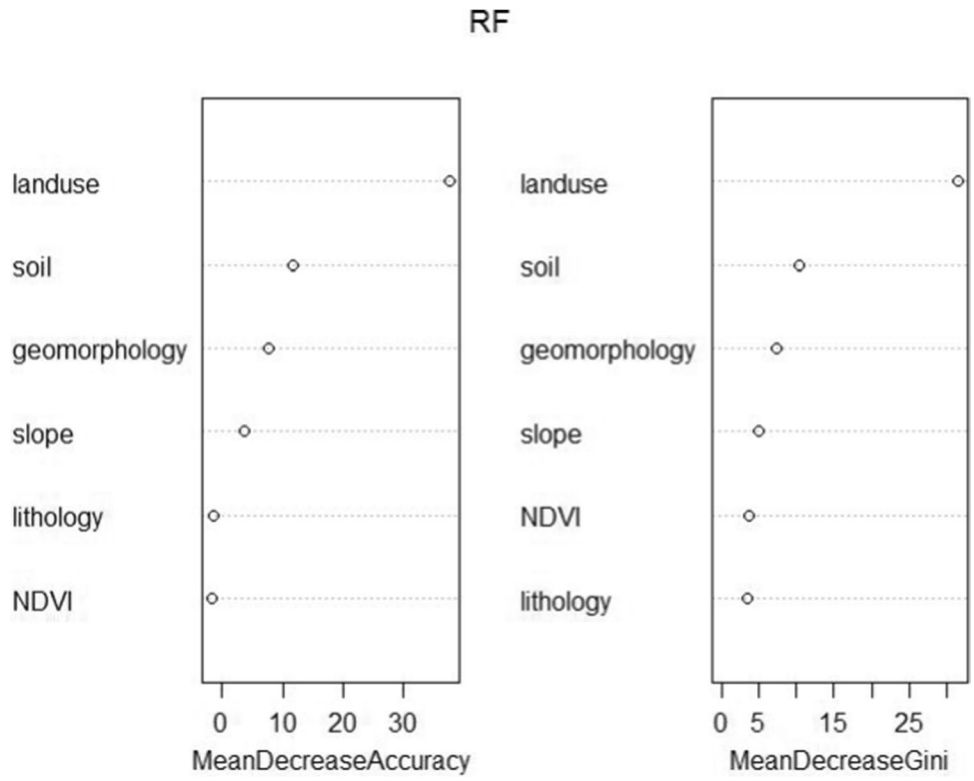

Fig. 6 Mean accuracy reduction and Gini mean reduction using the random forest model

Table 4 Confusion matrix for random forest model: 0 = dust source absents, 1 = dust source present

	Predicted		
	0	1	Class error
Actual			
0	97	9	0.084
1	11	95	0.15

Source: Study findings

Table 5 Results of determining the degree of importance of effective variables in the MARS model

Factors	GCV	RSS
Land use	100	100
Geomorphology	79.8	85.3
Slope	76.3	79.2
Soil	74.8	68.7
Lithology	71.1	55.4
NDVI	57.9	53.6

Source: Study findings

settings include the maximum number of base functions in the advanced stage, the maximum order of interactions, and the smoothing parameter. It is of note that the maximum number of base functions and the maximum order of interactions are the user-defined parameters of the model. In the MARS model, in the advanced stage, all the basic functions are added to the model stepwise, and at the end of this stage, the generated model causes a high computational error. In the regression stage, we achieved the final model by removing the redundant base functions that have the least effect on creating DSA. With each adjustment, a model is estimated, and the best model is chosen based on the minimum squares of the estimation error (RSS) and the GCV value. These results were calculated using the earth function in the R software. The MARS model was optimized with 11 nodes out of 23 nodes containing 12 base functions with GCV: 0.1 and also 18 subcategories out of 29 subcategories of independent variables. The MARS model uses only the independent variables and removes the other variables.

The MARS model can also analyze susceptibility by distinguishing between high-impact low-impact variables using the GCV (generalized cross-validation) and RSS (sum of squares of error) and by determining the degree of importance of each. Table 5 shows the ineffective variables and the results of determining the degree of importance of the effective variables. Figure 2 shows the relative contribution of each of the input parameters of the model in terms of the GCV.

The results indicate the 100% relative participation of the land use variable in the construction of the final model. The RSS value for land use is 100, suggesting that if land use is removed from the model, the sum of the square of the error is the maximum. Therefore, the existence of this variable is essential and shows the major and more effective role of land use than other variables in creating DSA. Other variables including geomorphology, slope, soil, lithology, and NDVI

are in the next rank regarding their importance and impact. These results are not consistent with the study of Gholami et al. (2020a), who assessed the impact of land use on dust at a moderate level in Khuzestan province. However, the results are consistent with those of Boroughani et al (2020). Also, the results of this study are consistent with the results of Rahmati et al. (2020) who indicated that soil maps and land use have the greatest impact and have the least impact on the modeling of dust sources compared to factors such as geology and topography. The results indicate that dust storms exist in dust source areas with suitable surfaces that allow dust mobilization. Therefore, soil type and land use are prerequisites for soil erosion through the wind. A large part of the studied area is covered by playa, dry beds of seasonal rivers and wetlands, sand dunes, and flat areas without vegetation. Accordingly, bare soil is the main physical feature of the area. As emphasized in previous studies, these types of land use and natural land cover are susceptible to dust aerosol emissions when they are dry (Goudie 2018; Hahnenberger and Nicoll 2014; Sissakian et al. 2013; Rashki et al. 2013).

Dust source susceptibility mapping (DSSM)

After executing the models in the R software for observational data and generalizing the modeling process to the whole study area, the output is a file with two columns of 0 and 1. The 0 column means no DSA for each pixel, and the 1 column indicates the existence of DSA for each pixel. DSSM modeling results were converted to point files based on the coordinates of each pixel in the GIS software environment. Then, the final map was prepared in a point-to-raster format. Eventually, based on natural fractures, they were classified into 4 classes: low, medium, high, and very high susceptibility (Fig. 7). These classes are set as in earlier studies (Mosavi et al. 2020). The results show that areas associated with wetlands or rivers have a greater potential for dust emissions due to drying and aridity during long periods of drought (Li and Sokolik 2018; Boroughani et al. 2021). The overall status of the case study was determined by calculating the area of dust sensitivity classes. Figure 8 shows the area of each sensitivity class and the DSA validation percentage of the dust source susceptibility map.

The results of the LR algorithm showed that 7.8% of the research area is in the low susceptibility area, and more than 68% falls in the very high susceptibility area. The results also indicate that most of the DSA (81.6%) are in the areas with high susceptibility. Based on the obtained results, more than 88% of DSA were placed in areas with high and very high susceptibility. The results presented in this study are in agreement with those reported by Gholami et al. (2020b). These researchers reported that a large part (> 80.0%) of the study area is susceptible to dust emissions and is classified as high and very high susceptibility classes. Examining the class area of the dust susceptibility map using an RF algorithm showed that about 70% of the DSAs are located at the class level in the classes with very high susceptibility. The MARS model also showed that more than 80% of the DSAs fall into two classes of high and very high susceptibility.

In all three models, high and very high susceptibility classes covered a large percentage of the research area. The highest percentage of DSA was also in this susceptibility category. In the RF and March models, very sensitive layers generally covered a smaller portion of the case study. Compared to the LR model, the DSA percentage in the high sensitivity class was higher in the MARS and RF models, suggesting the higher accuracy and more accurate implementation of these two models than the LR model. These findings, consistent with those of other results, show that RF allows more detailed spatial mapping of dust source susceptibility compared to other machine learning algorithms (Rahmati et al. 2020; Boroughani et al. 2020; Gholami et al. 2019; Darvand et al. 2021; Ebrahimi-Khusfi et al. 2021).

Validation of prepared maps is an essential step developing and identifying sensitive areas and their sources (Crawford et al. 2021). The classification is generally characterized as excellent for ROC values between 0.9 and 1.0, good for 0.8–0.9, good for 0.7–0.8, average for 0.6–0.7, and weak for 0.5–0.6 (Yesilnacar 2005). In this research, 30% of the DSAs were used for the evaluation or testing phase (called the prediction rate), and 70% for the modeling or training phase (called the success rate). As mentioned, ROC, AUC, and RMSE were used to validate the models. The validation of the models run based on 30%test data showed that RF, MARS, and LR models had AUC values of 0.94, 0.89, and 0.78, respectively. In addition, the validation results of these models using the training data showed the AUCs of0.92, 0.86, and 0.76 for the RF, MARS, and LR models, respectively. This result is consistent with previous studies that identified an RF with higher accuracy than other machine learning models for the spatial modeling of dust emission risks and source identifications (Boroughani et al. 2020; Ebrahimi-Khusfi et al. 2021; Gholami et al. 2019). The result is also consistent with those of Rahmati et al. research (2020), who identified sources of dust aerosol using a new framework based on remote sensing and modeling. Our results showed that the highest potential source of dust detected by the RF is in eastern Iran. Based on the RMSE criterion, RF outperformed the other models significantly. Table 6 shows the AUC and RMSE values in the training and validation phases of all the models. In addition, Fig. 9 shows the evaluation results of the models.

Like any other study, this study had some limitations. As the study area was located the Iran and Iraq border, it was very difficult to prepare effective layers because the countries' scales and preparation methods were different.

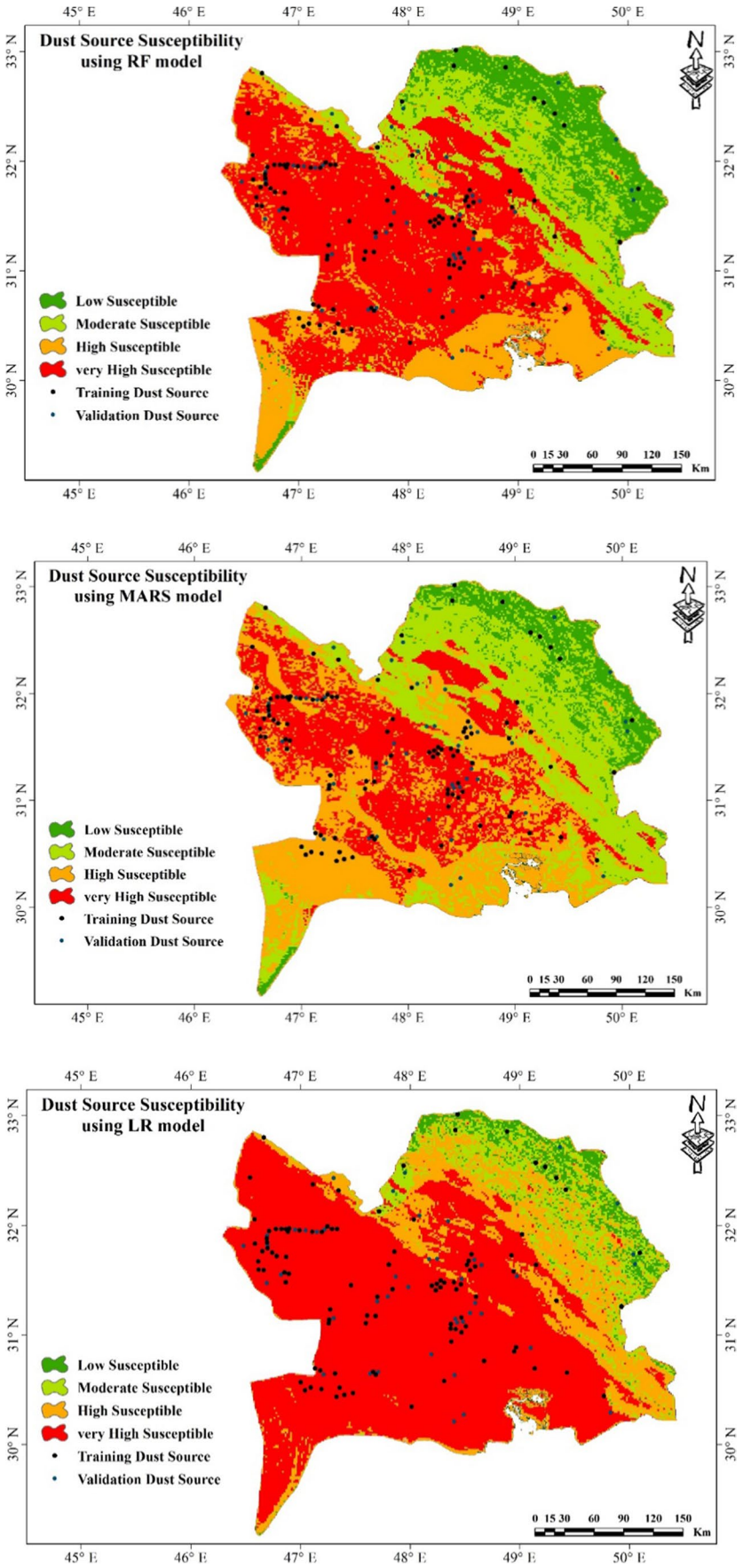

Fig. 7 DSSMs are produced by RF, MARS, and LR models

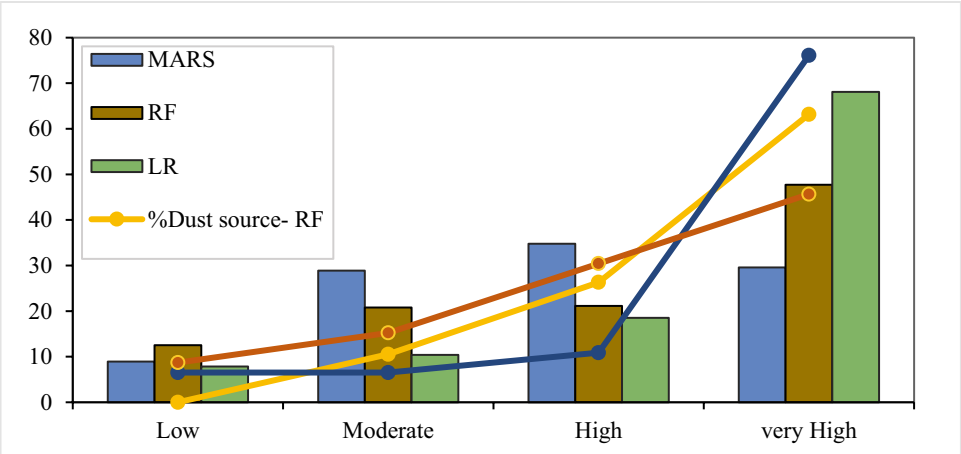

Fig. 8 Percentage of the area of sensitivity classes and percentage of the number of dust sources in the validation stage

Table 6 Area under the curve (AUC) and root mean square error (RMSE) values in the training and validation phases all of the models

Phases	Models	AUC (%)	RMSE
Training	RF	94	0.021
	MARS	89	0.032
	LR	78	0.05
Validation	RF	92	0.038
	MARS	86	0.062
	LR	76	0.078

Source: Study findings

Conclusion

This research aimed to integrate remote sensing and machine learning techniques for spatial mapping of the earth's sensitivity to dust diffusion in a very important DSA in the Iran and Iraq border. For this purpose, DSA was identified using MODIS satellite images and the Miller method. Then, the effective factors and dust source susceptibility maps were prioritized using LR methods, MARS, and RF. For this purpose, six independent variables (i.e., soil, lithology, slope, vegetation index, geomorphology units, and land use) were used as effective factors in creating the DSA. Considering that a part of the studied area was in Iraq, it was not possible to visit the field and use all the factors affecting the dust. The MARS, RF, and LR models showed that the highest DSA percentage falls into the very sensitive class. The implementation of all three models also showed that the land use and NDVI factor had the greatest and lowest impact on dust vulnerability in the study area, respectively. Evaluating these models using the ROC method showed that the RF, LR, and MARS models fall in the excellent, good, and very good categories. The RF with an AUC of 0.94 had a higher performance than the other two methods. In addition, RF outperformed the other models significantly based on the RMSE criterion. This research showed that climate change, drought, war and military operations, surface water control, diversion of rivers, and dam projects make

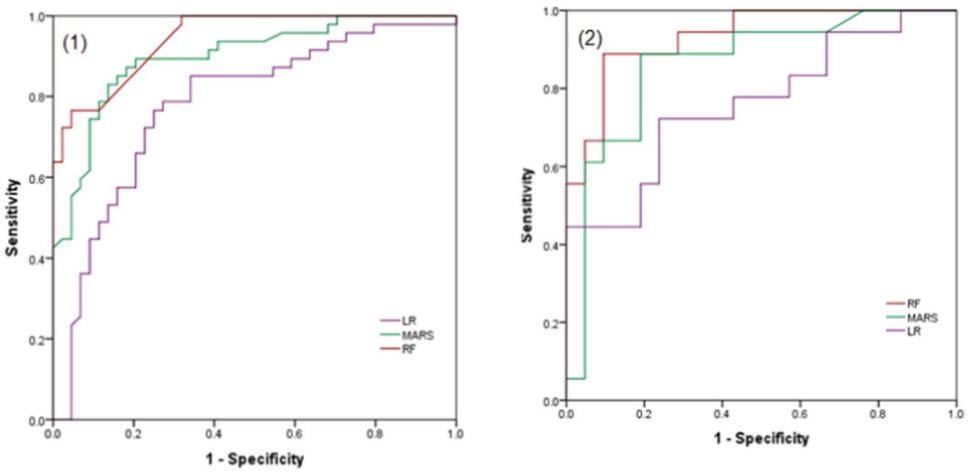

Fig. 9 (1) The success rate curve and (2) the predictive rate curve for the susceptibility maps produced in this research for all models

a large portion of the region to be highly sensitive to dust. The outputs of this model can be useful for planners and managers to control and reduce the risk of negative dust consequences. Future studies could work to prepare spatial maps of various environmental hazards, especially wind erosion, and predict the earth's sensitivity to dust emissions. Given the high potential impact of dust particles in many parts of Iran, we suggest extending, future research on dust source sensitivity to other regions.

Author contribution All authors contributed to the study conception and design. Material preparation, data collection and analysis were performed by Sima Pourhashemi, Mohammad Ali Zangane Asadi and Mahdi Boroughani. The first draft of the manuscript was written by Sima Pourhashemi and Mahdi Boroughani and all authors commented on previous versions of the manuscript. All authors read and approved the final manuscript.

Funding This work was supported by Mohammad Ali Zangane Asadi (Grant) from Hakim Sabzevari University.

Data availability The data that support the findings of this study are available from the corresponding author, Mohammad Ali Zangane Asadi, upon reasonable request.

Declarations

Ethics approval and consent to participate Not applicable.

Consent for publication The authors have not submitted the manuscript to a preprint server before submitting it to Environmental Science and Pollution Research. We confirm that this manuscript has not been published elsewhere and is not under consideration by another journal. All authors have approved the manuscript and agreed with its submission to Environmental Science and Pollution Research.

Conflict of interest The authors declare no competing interests.

References

Abyat A, Azhdari A, Kia HA, Joudaki M (2019) Khuzestan plain continental sabkhas, southwest Iran. Carbonates Evaporites 34(4):1469–1487

Akbari M, Bashiri M, Rangavar A (2017) Application of Data Mining Algorithms to Appreciate Sensitivity and Spatial Zoning Prone to Floating View in Khorasan Razavi Display Basins. J Environ Erosion Res 7(26):16–42

Al-Dousari A, Doronzo D, Ahmed M (2017) Types, indications and impact evaluation of sand and dust storms trajectories in the Arabian Gulf. Sustainability 9(9):1526

Alilou H, Rahmati O, Singh VP, Choubin B, Pradhan B, Keesstra S, Sadeghi SH (2019) Evaluation of watershed health using Fuzzy-ANP approach considering geo-environmental and topo-hydrological criteria. J Environ Manage 232:22–36

Arabameri A, Chandra Pal S, Rezaie F, Chakrabortty R, Saha A, Blaschke T, Di Napoli M, Ghorbanzadeh O, Thi Ngo PT (2022) Decision tree based ensemble machine learning approaches for landslide susceptibility mapping. Geocarto International 37(16):4594–4627

Arkian F (2017) Long-term variations of aerosols concentration over ten populated cities in iran based on satellite data. Hydrol Curr Res 8https://doi.org/10.4172/2157-7587.1000274

Baddock MC, Ginoux P, Bullard JE, Gill TE (2016) Do MODIS-defined dust sources have a geomorphological signature? Geophys Res Lett 43(6):2606–2613

Boloorani AD, Kazemi Y, Sadeghi A, Shorabeh SN, Argany M (2020) Identification of dust sources using long term satellite and climatic data: A case study of Tigris and Euphrates basin. Atmos Environ. https://doi.org/10.1016/j.atmosenv.2020.117299

Boroughani M, Hashemi H, Hosseini SH, Pourhashemi S, Berndtsson R (2019) Desiccating Lake Urmia: a new dust source of regional importance. IEEE Geosci Remote Sens Lett 17(9):1483–1487

Boroughani M, Pourhashemi S, Hashemi H, Salehi M, Amirahmadi A, Asadi MAZ, Berndtsson R (2020) Application of remote sensing techniques and machine learning algorithms in dust source detection and dust source susceptibility mapping. Eco Inform 56:101059

Boroughani M, Pourhashemi S, Gholami H, Kaskaoutis DG (2021) Predicting of dust storm source by combining remote sensing, statistic-based predictive models and game theory in the Sistan watershed, southwestern Asia. J Arid Land 13(11):1103–1121

Boroughani M, Mohammadi M, Mirchooli F, Fiedler S (2022) Assessment of the impact of dust aerosols on crop and water loss in the Great Salt Desert in Iran. Comput Electron Agric 192:106605

Cao H, Liu J, Wang G, Yang G, Luo L (2015) Identification of sand and dust storm source areas in Iran. Journal of Arid Land 7(5):567–578

Chaudhary A, Mriganka Sh, Bhupendra SA, Gopal SR (2021) Ageratina adenophora and Lantana camara in Kailash Sacred Landscape, India: Current distribution and future climatic scenarios through modeling. PLoS One 16(5):e0239690

Chen X, Chen W (2021) GIS-based landslide susceptibility assessment using optimized hybrid machine learning methods. CATENA 196:104833

Crawford MM, Dortch JM, Koch HJ, Killen AA, Zhu J, Zhu Y, Bryson LS, Haneberg WC (2021) Using landslide-inventory mapping for a combined bagged-trees and logistic-regression approach to determining landslide susceptibility in eastern Kentucky, USA. Q J Eng Geol Hydrogeol 54(4)

Darvand S, Khosravi H, Keshtkar H et al (2021) Comparison of machine learning models to prioritize susceptible areas to dust production. J Range Watershed Manag 74:53–68

Dube F, Nhapi I, Murwira A, Gumindoga W, Goldin J, Mashauri DA (2014) Potential of weight of evidence modelling for gully erosion hazard assessment in Mbire District-Zimbabwe. Phys Chem Earth, Parts a/b/c 67:145–152

Ebrahimi-khusfi Z, Taghizadeh-mehrjardi R, Mirakbari M (2021) Evaluation of machine learning models for predicting the temporal variations of dust storm index in arid regions of Iran. Atmos Pollut Res 12:134–147. https://doi.org/10.1016/j.apr.2020.08.029

Ebrahimi-Khusfi Z, Nafarzadegan AR, Dargahian F (2021) Predicting the number of dusty days around the desert wetlands in southeastern Iran using feature selection and machine learning techniques. Ecol Ind 125https://doi.org/10.1016/j.ecolind.2021.107499

Feng C, Janssen H (2018) Hygric properties of porous building materials (III): Impact factors and data processing methods of the capillary absorption test. Build Environ 134:21–34

Feuerstein S, Schepanski K (2019) Identification of dust sources in a Saharan dust hotspot and their implementation in a dust-emission model. Remote Sens 11(1):4

Francis DBK, Flamant C, Chaboureau JP, Banks J, Cuesta J, Brindley H, Oolman L (2017) Dust emission and transport over Iraq associated with the summer Shamal winds. Aeol Res 24:15–31

Francis D, Chaboureau J-P, Nelli N, Cuesta J, Alshamsi N, Temimi M, Pauluis O, Xue L (2021) Summertime dust storms over the Arabian Peninsula and impacts on radiation, circulation, cloud development and rain. Atmos Res 250:105364. https://doi.org/10.1016/j.atmosres.2020.105364

Friedman JH (1991) Multivariate adaptive regression splines. Ann Stat 19:1–67

Genuer R, Poggi J-M, Tuleau-Malot C, Villa-Vialaneix N (2017) Random forests for big data. Big Data Res 9:28–46

Gholami H, Rahimi S, Fathabadi A, Habibi S, Collins AL (2020a) Mapping the spatial sources of atmospheric dust using GLUE and Monte Carlo simulation. Sci Total Environ 723:138090

Gholami H, Mohamadifar A, Collins AL (2020b) Spatial mapping of the provenance of storm dust: application of data mining and ensemble modelling. Atmos Res 233:104716

Gholami H, Mohammadifar A, Malakooti H, Esmaeilpour Y, Golzari S, Mohammadi F, Li Y, Song Y, Kaskaoutis DG, Fitzsimmons KE, Collins AL (2021) Integrated modelling for mapping spatial sources of dust in central Asia-An important dust source in the global atmospheric system. Atmos Pollut Res 12(9):101173

Gholami H, Mohammadifar A, Collins AL (2019) Spatial mapping of the provenance of storm dust: application of data mining and ensemble modelling Hamid. Atmos Res 104716https://doi.org/10.1016/j.atmosres.2019.104716

Giang PQ, Trang NTM, Anh TTH, Binh NT (2020) Prediction of economic loss of rice production due to flood inundation under climate change impacts using a modeling approach: A case study in Ha Tinh Province, Vietnam. Clim Chang 6:52–63

Gomila R (2021) Logistic or linear? Estimating causal effects of experimental treatments on binary outcomes using regression analysis. J Exp Psychol Gen 150(4):700

Goossens D, Buck B (2014) Dynamics of dust clouds produced by off-road vehicle driving. J Earth Sci Geotech Eng 4(2):1–21

Goudie AS (2018) Human impact on the natural environment. John Wiley & Sons

Guo P, Lam JC, Li VO (2018) A novel machine learning approach for identifying the drivers of domestic electricity users' price responsiveness. University of Cambridge, Faculty of Economics

Hahnenberger M, Nicoll K (2014) Geomorphic and land cover identification of dust sources in the eastern Great Basin of Utah, USA. Geomorphology 204:657–672

Hao F, Tan W, Jiang LI, Zhang L, Zhao X, Zou Y, Hu Y, Luo X, Jiang X, McIntyre RS, Tran B (2020) Do psychiatric patients experience more psychiatric symptoms during COVID-19 pandemic and lockdown? A case-control study with service and research implications for immunopsychiatry. Brain Behav Immun 87:100–106

Hassangavyar MB, Damaneh HE, Pham QB, Linh NTT, Tiefenbacher J, Bach QV (2022) Evaluation of re-sampling methods on performance of machine learning models to predict landslide susceptibility. Geocarto International 37(10):2772–2794

Heald CL, Spracklen DV (2015) Land use change impacts on air quality and climate. Chem Rev 115(10):4476–4496

Heidarian P, Azhdari A, Joudaki M, Khatooni JD, Firoozjaei SF (2018) Integrating remote sensing, GIS, and sedimentology techniques for identifying dust storm sources: a case study in Khuzestan, Iran. J Indian Soc Remote Sens 46(7):1113–1124

Hong H, Naghibi SA, Pourghasemi HR, Pradhan B (2016) GIS-based landslide spatial modeling in Ganzhou City, China. Arab J Geosci 9(2):1–26. https://doi.org/10.1007/2Fs12517-015-2094-y

Javadian M, Behrangi A, Sorooshian A (2019) Impact of drought on dust storms: case study over Southwest Iran. Environ Res Lett 14(12):124029

Jiang C, Fan W, Yu N, Liu E (2021) Spatial modeling of gully head erosion on the Loess Plateau using a certainty factor and random forest model. Sci Total Environ 783:147040

Jiao P, Wang J, Chen X, Ruan J, Ye X, Alavi AH (2021) Next-generation remote sensing and prediction of sand and dust storms: State-of-the-art and future trends. Int J Remote Sens 42(14):5277–5316

Kandakji T, Thomas E, Jeffrey A (2020) Identifying and characterizing dust point sources in the southwestern United States using remote sensing and GIS. Geomorphology 353:107019

Kandakji T, Gill T, Lee J (2021) Drought and land use/land cover impact on dust sources in Southern Great Plains and Chihuahuan Desert of the U.S.: Inferring anthropogenic effect. Sci Total Environ 755:1–13

Karimi B, Samadi S (2019) Mortality and hospitalizations due to cardiovascular and respiratory diseases associated with air pollution in Iran: A systematic review and meta-analysis. Atmos Environ 198:438–447

Kok JF, Ridley DA, Zhou Q, Miller RL, Zhao C, Heald CL, Ward DS, Albani S, Haustein K (2017) Smaller desert dust cooling effect estimated from analysis of dust size and abundance. Nat Geosci 10(4):274–278

Lee EH, Sohn BJ (2011) Recent increasing trend in dust frequency over Mongolia and Inner Mongolia regions and its association with climate and surface condition change. Atmos Environ 45(27):4611–4616

Lee JA, Gill TE, Mulligan KR, Acosta MD, Perez AE (2009) Land use/land cover and point sources of the 15 December 2003 dust storm in southwestern North America. Geomorphology 105(1–2):18–27

Lee J, Shi YR, Cai C, Ciren P, Wang J, Gangopadhyay A, Zhang Z (2021) Machine learning based algorithms for global dust aerosol detection from satellite images: inter-comparisons and evaluation. Remote Sens 13(3):456

Lee-Sunmin Kim JC, Jung HS, Lee MJ, Lee S (2017) Spatial prediction of flood susceptibility using random-forest and boosted-tree models in Seoul metropolitan city, Korea. Geomat Nat Hazard Risk 8:1185–1203

Li L, Sokolik IN (2018) The dust direct radiative impact and its sensitivity to the land surface state and key minerals in the WRF-Chem-DuMo Model: a case study of dust storms in Central Asia. J Geophys Res: Atmospheres 123(9):4564–4582

Lin X, Chang H, Wang K, Zhang G, Meng G (2020) Machine learning for source identification of dust on the Chinese Loess Plateau. Geophys Res Lett 47(21):e2020GL088950

Liu Y, Wang G, Hu Z, Shi P, Lyu Y, Zhang G, Gu Y, Liu Y, Hong C, Guo L, Hu X, Yang Y, Zhang X, Zheng H, Liu L (2020) Dust storm susceptibility on different land surface types in arid and semiarid regions of northern China. Atmos Res 243:1–10

Manap MA, Nampak H, Pradhan B, Lee S, Sulaiman WNA, Ramli MF (2014) Application of probabilistic-based frequency ratio model in groundwater potential mapping using remote sensing data and GIS. Arab J Geosci 7(2):711–724. https://doi.org/10.1007/s12517-012-0795-z

Martinello C, Cappadonia C, Conoscenti C, Agnesi V, Rotigliano E (2021) Optimal slope units partitioning in landslide susceptibility mapping. J Maps 17(3):152–162

Martinez-Garcia A, Rosell-Mele A, Jaccard SL, Geibert W, Sigman DM, Haug GH (2011) Southern Ocean dust–climate coupling over the past four million years. Nature 476(7360):312–315

Martinich J, Roman H, Mickley LJ (2019) Effects of increasing aridity on ambient dust and public health in the US southwest under climate change. GeoHealth 3(5):127–144

Middleton NJ (2017) Desert dust hazards: a global review. Aeolian Res 24:53–63

Miller SD (2003) A consolidated technique for enhancing desert dust storms with MODIS. Geophys Res Lett 30(20)

Mosavi A, Golshan M, Janizadeh S et al (2020) Ensemble models of GLM, FDA, MARS, and RF for flood and erosion susceptibility

mapping: a priority assessment of sub-basins. Geocarto Int. https://doi.org/10.1080/10106049.2020.1829101
Namdari S, Karimi N, Sorooshian A, Mohammadi G, Sehatkashani S (2018) Impacts of climate and synoptic fluctuations on dust storm activity over the Middle East. Atmos Environ 173:265–276
Namdari M, Lee CS, Haghighat F (2021) Active ozone removal technologies for a safe indoor environment: a comprehensive review. Build Environ 187:107370
Nandi A, Shakoor A (2010) A GIS-based landslide susceptibility evaluation using bivariate and multivariate statistical analyses. Eng Geol 110(1–2):11–20
Nhu VH, Mohammadi A, Shahabi H, Ahmad BB, Al-Ansari N, Shirzadi A, Geertsema M, Kress VR, Karimzadeh S, Valizadeh Kamran K, Chen W (2020) Landslide detection and susceptibility modeling on cameron highlands (Malaysia): a comparison between random forest, logistic regression and logistic model tree algorithms. Forests 11(8):830
O'brien RM (2007) A caution regarding rules of thumb for variance inflation factors. Qual Quant 41(5):673–690
Park S, Hamm S-Y, Jeon H-T, Kim J (2017) Evaluation of logistic regression and multivariate adaptive regression spline models for groundwater potential mapping using R and GIS. Sustainability 9:1157. https://doi.org/10.3390/su9071157
Quevedo RP, Maciel DA, Uehara TDT, Vojtek M, Renno CD, Pradhan B, Vojtekova J, Pham QB (2021) Consideration of spatial heterogeneity in landslide susceptibility mapping using geographical random forest model. Geocarto International 1–24
Rahmati O, Mohammadi F, Ghiasi SS, Tiefenbacher J, Moghaddam DD, Coulon F, Nalivan OA, Bui DT (2020) Identifying sources of dust aerosol using a new framework based on remote sensing and modelling. Sci Total Environ 737:139508
Rashki A, Kaskaoutis DG, Goudie AS, Kahn RA (2013) Dryness of ephemeral lakes and consequences for dust activity: the case of the Hamoun drainage basin, southeastern Iran. Sci Total Environ 463:552–564
Rashki A, Middleton NJ, Goudie AS (2021) Dust storms in Iran – Distribution, causes, frequencies and impacts. Aeol Res 48:1–17
Roy P, Chandra Pal S, Arabameri A, Chakrabortty R, Pradhan B, Chowdhuri I, Lee S, Tien Bui D (2020) Novel ensemble of multivariate adaptive regression spline with spatial logistic regression and boosted regression tree for gully erosion susceptibility. Remote Sens 12(20):3284
Schepanski K, Tegen I, Macke A (2012) Comparison of satellite based observations of Saharan dust source areas. Remote Sens Environ 123:90–97
Schonlau M, Zou RY (2020) The random forest algorithm for statistical learning. Stand Genomic Sci 20(1):3–29
Shaheen A, Wu R, Aldabash M (2020) Long-term AOD trend assessment over the Eastern Mediterranean region: a comparative study including a new merged aerosol product. Atmos Environ. https://doi.org/10.1016/j.atmosenv.2020.117736
Shano L, Raghuvanshi TK, Meten M (2021) Landslide hazard zonation using logistic regression technique: the case of Shafe and Baso catchments, Gamo highland, Ethiopia
Sissakian V, Al-Ansari N, Knutsson S (2013) Sand and dust storm events in Iraq. J Nat Sci 5(10):1084–1094
Soni M, Payra S, Verma S (2018) Particulate matter estimation over a semi arid region Jaipur, India using satellite AOD and meteorological parameters. Atmos Poll Res. https://doi.org/10.1016/j.apr.2018.03.001
Taheri F, Forouzani M, Yazdanpanah M, Ajili A (2020) How farmers perceive the impact of dust phenomenon on agricultural production activities: A Q-methodology study. J Arid Environ 173:104028
Vickery K, Eckardt F (2013) Dust emission controls on the lower Kuiseb River valley, central Namib. Aeolian Res 10:125–133. https://doi.org/10.1016/j.aeolia.2013.02.006
Walker AL, Liu M, Miller SD, Richardson KA, Westphal DL (2009) Development of a dust source database for mesoscale forecasting in Southwest Asia. J Geophys Res 114(18):1–24. https://doi.org/10.1029/2008JD011541
Wang L, Tremblay D, Zhang B, Han Y (2016) Fast and accurate collocation of the visible infrared imaging radiometer suite measurements with cross-track infrared sounder. Remote Sens 8(1):76. https://doi.org/10.3390/rs8010076
Wang L, Wu C, Gu X, Liu H, Mei G, Zhang W (2020) Probabilistic stability analysis of earth dam slope under transient seepage using multivariate adaptive regression splines. Bull Eng Geol Env 79(6):2763–2775
Wang H, Zhang L, Yin K, Luo H, Li J (2021a) Landslide identification using machine learning. Geosci Front 12(1):351–364
Wang T, Ma H, Liu J, Luo Q, Wang Q, Zhan Y (2021b) Assessing frost heave susceptibility of gravelly soils based on multivariate adaptive regression splines model. Cold Reg Sci Technol 181:103182
Wu C, Lin Z, He J, Zhang M, Liu X, Zhang R, Brown H (2016) A process-oriented evaluation of dust emission parameterizations in CESM: Simulation of a typical severe dust storm in E ast A sia. J Adv Model Earth Syst 8(3):1432–1452
Wu H, Lin A, Xing X, Song D, Li Y (2021) Identifying core driving factors of urban land use change from global land cover products and POI data using the random forest method. Int J Appl Earth Obs Geoinf 103:102475
Yang L, Jin S, Danielson P, Homer C, Gass L, Bender SM, Case A, Costello C, Dewitz J, Fry J, Funk M, Granneman B, Liknes GC, Rigge M, Xian G (2018) A new generation of the United States National Land Cover Database: requirements, research priorities, design, and implementation strategies. ISPRS J Photogramm Remote Sens 146:108–123
Yesilnacar EK (2005) The application of computational intelligence to landslide susceptibility mapping in Turkey. University of Melbourne, Department, 200
Yu H, Chin M, Yuan T, Bian Hremer LA, Prospero JM, Omar A, Winker D, Yang Y, Zhang Y, Zhang Z, Zhao C (2015) The fertilizing role of African dust in the Amazon rainforest: a first multiyear assessment based on CALIPSO LIDAR observations. Geophys Res Lett 42:1984–1991
Zhang S, Li C, Peng J, Peng D, Xu Q, Zhang Q, Bate B (2021) GIS-based soil planar slide susceptibility mapping using logistic regression and neural networks: a typical red mudstone area in southwest China. Geomat Nat Haz Risk 12(1):852–879